Chapter 6

Phase Unbalance and PAR constrained: Optimal Scheduling of PHEVs and DGs

6.1 Introduction

The last two chapters deal with optimal active power scheduling of PHEVs in presence of local DER modules considering single phase equivalent single phase distribution system. This chapter investigates the optimal active and reactive power scheduling of (Plug-in-Hybrid Electric Vehicles (PHEVs) and Distributed Generations (DGs) in unbalanced distribution system, considering unbalance and Peak-to-Average Ratio (PAR) constraints.

The uncoordinated and unpredictable cluster of charging/discharging phenomena of EV causes increased phase currents in distribution system resulting in phase unbalance and may lead to tripping of the distribution system. The increase in penetration of EV/PHEVs may affect the parameters such as voltage deviations, quality of supply, power losses and transformers aginging in distribution system. Maintaining the techno-economical constraints and phase balance of distribution networks throughout the day is a challenging problem. The distribution system operators experience high current and voltage unbalance due to the planning approach which are done normally on a single phase basis. As technology matures toward charging technology, electric vehicle chargers could provide active and reactive power simultaneously without degrading State-of-Charge (SOC) of batteries. Hence, the optimal active and reactive power scheduling of PHEVs and DGs can be used to mitigate the phase unbalance, voltage deviation and peak demand due to unpredictable loading pattern of PHEVs on three phase unbalanced distribution system. A possible formulation would be to use a multi-objective function including cost, phase balancing and load flattening as components. From other perspective, formulation could be to use cost as main objective and unbalancing and PAR (load flattening) as constraints. In practical scenario the VPPs would like to prefer load flattening and unbalance as constrained, because the situation can allow them to appropriately tune the amount of unbalance factor and PAR viz a viz. cost. Also, the cost benefit analysis of PAR and unbalance can be performed.

In this chapter, adaptation of co-ordinated active and reactive power scheduling of DGs and EVCS is investigated in three sequential stages. In the first stage the uncertainties related to driving habits of PHEVs is modelled by Monte-Carlo Simulation (MCS) technique and SOC profiles of all PHEVs has been obtained as discussed in chapter-3. Further, in second stage, a Non Linear Program (NLP) mathematical model and selection of candidate site for DGs installation and EVCS have been considered. In the last stage, formulation of a mathematical model which aims the minimize VPPs operational cost considering current and voltage unbalance and PAR constraints is performed. Moreover, a dependencies of cost and losses are investigated with helps of pay-off tables. The pay-off tables relates unbalance factor and PAR to cost and losses. To simulate the model of proposed idea, a IEEE-25 bus three phase unbalanced system is adopted and for these investigations all the analytical simulations are performed in GAMS/MATLAB environment.

6.2 Problem Formulation

This section presents the problem formulation using cost as the primary objective, with phase unbalance and load flattening as constraints. In a practical scenario, for the techno-economic operation, VPPs would like to prefer load flattening and unbalance as constrained, because the situation can allow them to tune the amount of unbalance factor and PAR appropriately. Also, the cost benefit analysis of PAR and unbalance can be performed. The time step of one hour is taken for the problem formulation.

6.2.1 Objective function

The proposed optimisation model aims to minimise the energy cost of VPPs and can be represented as,

$$F = Min[f].$$

The objective function can be mathematically formulated as follows.

$$\begin{aligned} f = \sum_{ph=a,b,c} \sum_{h=1}^{24} \Bigg(\Big[\sqrt{P_{CPG}^2(t) + Q_{CPG}^2(h)} \Big] CS_{CPG}(h) + \sum_{e=1}^{N_{PHEV}} \sum_{c=1}^{N_{EVCS}} P_{V2G}(e,c,h) \\ k_{PHEV} C_d(h) + \sum_{d=1}^{N_{DG}} P_{DG}(d,h) k_{DG} C_{DG} + \Big[\sum_{e=1}^{N_{PHEV}} \sum_{c=1}^{N_{EVCS}} Q_{V2G}(e,c,h) k_{PHEV} \\ + \sum_{d=1}^{N_{DG}} Q_{DG}(d,h) k_{DG} \Big] C_{RPC} \Bigg). \end{aligned} \tag{6.1}$$

Where, $P_{CPG(h)}$, $P_{DG}(h)$ and $P_{V2G}(h)$ are the power output from Conventional Power Generator (CPG), DG and PHEVs (in V2G mode) at time h respectively. $Q_{CPG}(h)$, Q_{DG} and Q_{V2G} are the reactive power output from CPG, DGS and PHEVs (V2G mode) respectively.

k_{DG} and k_{PHEV} are binary numbers (0,1) representing connection status of DGs and PHEVs. So, that if $k_{DG} = k_{PHEV} = 0$ which means the there is no exchange of power, whereas, if $k_{DG} = k_{PHEV} = 1$ which means there is an exchange of power between grid and DG/PHEVs.

Equation (6.1) describes the total energy cost of VPPs in terms of the active and reactive power scheduling. The first term of (6.1) shows the expenses from the conventional power generator, whereas second and third terms are related to injected active power and reactive power cost associated with EVCS and DGs.

6.2.2 Constraints

Power flow constraints at h^{th} hour

The active and reactive power balance constraints can be written as follows.

$$-P_{load}(h,k,ph) + P_{DG}(h,k,ph) - \sum_{c=1}^{N_{EVCS}} \sum_{e=1}^{N_{PHEV}} \big(y(c,e,k) \times (P_{G2V}(c,e,h) - P_{V2G}(c,e,h))\big) \leq \epsilon, \tag{6.2}$$

$$-Q_{load}(t,k,ph) + Q_{dg}(t,k,ph) - \sum_{c=1}^{N_{evcs}} \sum_{e=1}^{N_{phev}} ((y(c,e,k) \times Q_{g2v}(c,e,t) - Q_{v2g}(c,e,t)))) \leq \epsilon. \tag{6.3}$$

Equations (6.2) & (6.3) ensure the generation and load demand on distribution system should be matched at all times.

Phase current balance constraints

The phase current balance equation in terms of zero and negative sequence current are as follows.

$$-0.02 \leq I_0(h) \leq 0.02, \tag{6.4}$$

$$-0.02 \leq I_2(h) \leq 0.02, \tag{6.5}$$

where, $I_0(h)$ and $I_2(h)$ are the zero and negative sequence component of three phase current I_a, I_b and I_c respectively. $I_0(h)$ and $I_2(h)$ can be calculated using the following relation,

$$\begin{bmatrix} I_0(h) \\ I_1(h) \\ I_2(h) \end{bmatrix} = \begin{bmatrix} 1 & 1 & 1 \\ 1 & a^2 & a \\ 1 & a & a^2 \end{bmatrix} \begin{bmatrix} I_a \\ I_b \\ I_c \end{bmatrix}.$$

Where, $a = 1\angle 120^o$.

Equation (6.4) and (6.5) imposes the current unbalance constraint in distribution system.

Voltage unbalance constraints

The phase voltage balance equations in terms of Phase Voltage Unbalance Index (PVUI) are as follows,

$$-0.03 \leq PVUI \leq 0.03, \tag{6.6}$$

$$PVUI = Max[\Delta V_{ph=a,b,c}], \tag{6.7}$$

$$\Delta V_{ph=a,b,c} = \frac{V(i,h) - \overline{V}(i,h)}{\overline{V}(i,h)},$$

where,

$$\overline{V}(i,h) = \frac{1}{24} \sum_{ph=a,b,c} \sum_{i=1}^{N_B} \sum_{h=1}^{24} V(i,h,ph).$$

According to IEEE standard 1159-2009 [167], equation (6.6), the PVUI should be limited under ±3% (for mostly single phase loading) [167].

Peak-to-Average Ratio (PAR) constraints

PAR is one of the significant technical constraints for VPPs. However, PAR can not be forced to a desired value but needs to be adjusted to appropriate value for a feasible scheduling. The PAR constraints can be expressed as,

$$PAR = \frac{Max[P(h)]}{\overline{P}(h)},$$

$$Max[P(h)] \leq PAR_{max} \times \overline{P}(h). \tag{6.8}$$

Where,

$$P(h) = \sum_{i=1}^{N_B} \sum_{ph=a,b,c} \Bigg(P_{load}(i,ph,h) - P_{DG}(i,ph,h) - \sum_{e=1}^{N_{EVCS}} \sum_{e=1}^{N_{PHEV}} y(c,e,k)(P_{V2G}(c,e,h) - P_{G2V}(c,e,h)) \Bigg) + \sum_{ph=a,b,c} P_{loss}(h,ph)$$

Where, $PAR_{max} = 1.2$ is set as the maximum tolerable PAR in the network.

Equation (6.8) limits the peak demand to $PAR_{max} \times \overline{P}(t)$ at time t.

DG power output limits

The DGs active and reactive power range is restricted in constraint (6.9) & (6.10) as follows.

$$P_{DG-min}(d,ph,h) \leq P_{DG}(d,ph,h) \leq P_{DG-max}(d,ph,h), \tag{6.9}$$

$$Q_{DG-min}(d,ph,h) \leq Q_{DG}(d,ph,h) \leq Q_{DG-max}(d,ph,h). \tag{6.10}$$

Technical constraints on PHEVs

Following are the technical limit imposed on the PHEVs.

Equation (6.11) represents the PHEV's battery cannot be charged and discharge simultaneously.

$$P_{G2V} \times P_{V2G} = 0. \tag{6.11}$$

The charger capacity of PHEV is limited and is expressed as ,

$$\sqrt{P^2_{PHEV}(e,h) + Q^2_{PHEV}(e,h)} \leq S_{CH-max}. \tag{6.12}$$

SOC limits for the e^{th} PHEV can be expressed as,

$$SOC_{min}^{PHEV}(e) \leq SOC^{PHEV}(e,h) \leq SOC_{max}^{PHEV}(e). \tag{6.13}$$

Where, $SOC_{min}^{PHEV}(e)$ and $SOC_{max}^{PHEV}(e)$ are the minimum and maximum state-of-charge of battery.

The SOC balance equation for the e^{th} PHEV can be expressed as,

$$SOC^{PHEV}(e,h) = SOC^{PHEV}(e,h-1) + \frac{100}{BC_{PHEV}}\left(\eta_c P_{G2V}(c,e) - \frac{P_{V2G}(c,e)}{\eta_d}\right). \tag{6.14}$$

Dependency of the charging and discharging power of PHEVs on the SOC of the battery at an instant t can be expressed as,

$$\eta_c P_{g2v}(e,h) \leq min\left[P_{g2v,max}, \left(\frac{BC_{phev}(e)}{100}\left(SOC_{max}(e) - SOC(e,h-1)\right)\right)\right], \tag{6.15}$$

$$\frac{P_{v2g}(e,h)}{\eta_d} \leq min\left[P_{v2g,max}, \left(\frac{BC_{phev}(e)}{100}\left(SOC(e,h-1) - SOC_{min}(e)\right)\right)\right]. \tag{6.16}$$

The constraint for PHEVs to get maximum possible SOC at departure time $SOC_{t_{dep}}(e)$ of e^{th} PHEV can be given as follows,

$$SOC_{t_{dep}}^{PHEV}(e) = \left[min\left(100, (SOC_{t_{arr}}^{PHEV}(e) + \frac{P_{G2V-max}(e)}{BC_{PHEV})} \times \Delta T \times 100)\right)\right]. \tag{6.17}$$

Where,

$$\Delta T = \begin{cases} (t_{dep} - t_{arr}) & t_{arr} < t_{dep} \\ 24 + (t_{dep} - t_{arr}) & t_{arr} > t_{dep}. \end{cases} \tag{6.18}$$

6.3 Candidate Bus Selection of EVCS and DGs

A mathematical framework for the siting problem for all DGs and EVCS is developed in this section. The candidate bus selection for DGs and EVCS in distribution system plays a significant role in mitigating the adverse effects on the distribution system such as a reduction in operating cost, reduction in energy losses, voltage profile and energy balance problem. In this work, the selection of candidate bus for DGs and EVCS is to minimise operating cost of VPPs.

Mathematically, this can be formulated as follows,

$$\text{Minimize:} \quad S. \tag{6.19}$$

$$S = \sum_{h=1}^{24} \sum_{ph=a,b,c} \Bigg(P_{CPG}(h) \times C_c(h) + \sum_{d=1}^{N_{DG}} P_{DG}(d,h) x(d,ph,k) \times C_{DG} + \sum_{e=1}^{N_{PHEV}} \sum_{c=1}^{N_{EVCS}} P_{V2G}(e,c,h) y(c,ph,k) \times C_d(h) \Bigg). \tag{6.20}$$

Subject to:

$$\sum x(d,ph,k) = 5, \tag{6.21}$$

$$\sum y(c,ph,k) = 10. \tag{6.22}$$

Where,

$$0 \leq x(d,ph,k) \leq 1, \tag{6.23}$$

$$0 \leq y(c,ph,k) \leq 1. \tag{6.24}$$

$$\text{if} \begin{Bmatrix} (k \neq j, d_1 = d_2) \\ (k = j, ph_1 = ph_2) \\ (d_1 \neq d_2) \end{Bmatrix} = \begin{matrix} x(k,ph_1,d_1) \\ \times x(j,ph_2,d_2) = 0, \end{matrix}$$

$$\text{if} \begin{Bmatrix} (k \neq j, c_1 = c_2) \\ (k = j, ph_1 = ph_2) \\ (c_1 \neq c2) \end{Bmatrix} = \begin{matrix} y(k,ph_1,c_1) \\ \times x(j,ph_2,c_2) = 0. \end{matrix}$$

$$P_{DG}(h) \leq P_{DG-max}, \tag{6.25}$$

$$P_{EVCS}(h) \leq P_{EVCS-max}. \tag{6.26}$$

The model described in equation (6.21) and (6.22) are linked with the limit on a maximum number of DGs and EVCS. Further, the following two equation ensures that there are no two DGs or two EVCS installed on the same node of the distribution system. Equation (6.23) and (6.24) force the limit regarding the number of DGs and EVCSs. Maximum power limits of DGs and EVCS are represented by (6.25) and (6.26).

6.4 System Model

The IEEE 25-bus three-phase unbalanced distribution system network has been considered for this study. The load data, line connectivity and impedance for a different type of conductor used in the distribution system are adopted from ref. [168]. The detailed system specification and data given in Appendix I. The distribution system is energised through a conventional power generator at which is connected at bus-1 Point of Common Coupling (PCC). The voltage at PCC is fixed at 1.05 p.u. The conventional loading on distribution system consists of a combination of mixed load (residential, commercial and industrial) [2] has been considered in this work. The distribution system adopted for the present study 150 PHEVs and similar five Wind Turbine (WTs) DGs have been considered.

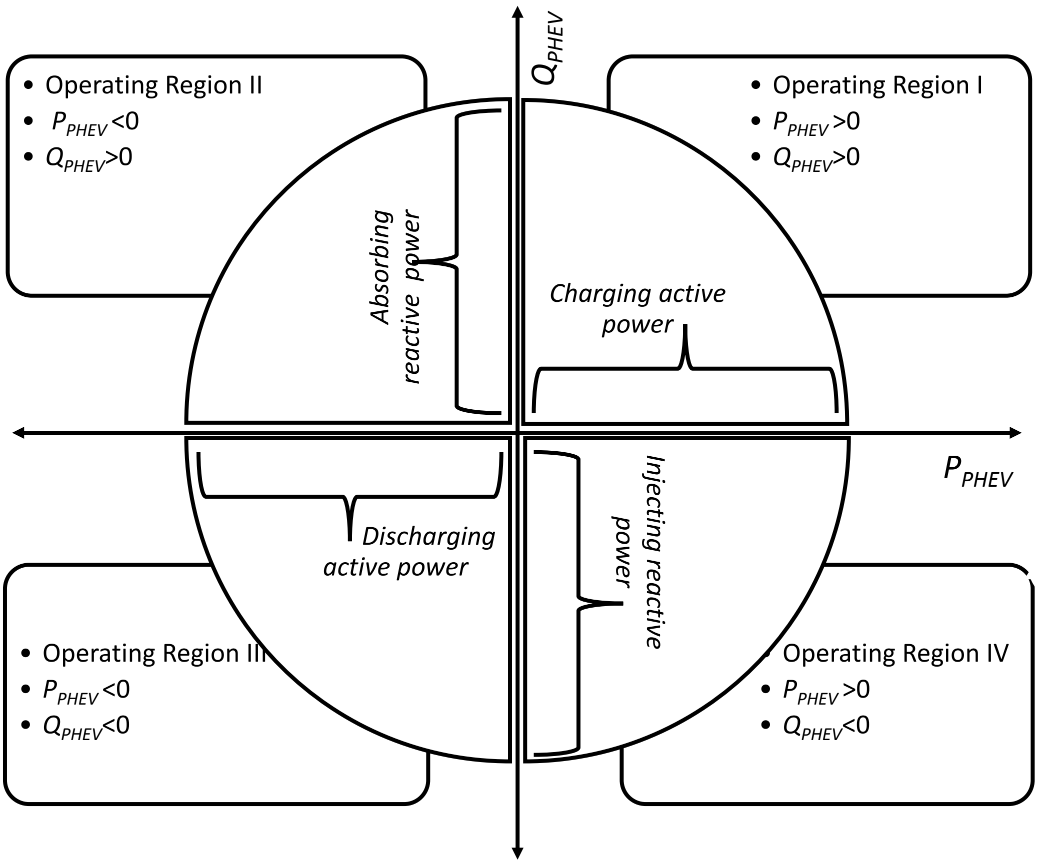

Figure 6.1: Single-phase PHEV charger operational characteristics

Fig. 6.1 shows the single-phase bidirectional charging characteristics [169] for charger installed at EVCS. EVs' battery chargers are often equipped with a 4-quadrant converter that can be enabled to exchange reactive power. Such smart charger circuit can adjust the exchange of reactive power to the distribution system by controlling the power factor of the charger.

The amount of active power drawn from the grid to charge the battery of the vehicle depends upon SOC, battery capacity, and the charging efficiency. The active power and reactive power can be calculated as follows.

$$P_{phev-e} = \left(\frac{1 - \frac{SOC}{100}}{\eta} \right) \times BC_{phev}, \tag{6.27}$$

and,

$$Q_{phev-e} = P_{phev-e}(t)\sqrt{\frac{1-\phi^2}{\phi}}.$$

Where, BC_{phev} is the battery capacity, η is the charger efficiency, P_{phev-e} and Q_{phev-e} are active and reactive power respectively for e^{th} PHEV at time t.

The tariff of energy is specified in terms of active power. According to [170], based on basic triangular relationship between P, Q and S, the energy tariff (for conventional power generator) in €/MVA can be derived as €/MVA=€/MW $\times$ p.f. Where $p.f$ is nominal power factor of conventional power generator source. The other forms of small explicit cost are neglected. When the conventional power generator source is operating at the nominal power factor 0.9, the capital cost in terms of MVA is $CS_{cpg}(t) = C_{cpg} \times 0.9$ €/MVA. The tariff of energy supplied by the utility to EVCS ($C_{cpg}(t)$) and cost paid by utility to the consumer for V2G mode of PHEVs ($C_{v2g}(t)$) is adopted from [164]. In this paper, it is assumed that reactive power exchange cost between utility to EVCS or DGs has been expressed in terms of reactive power compensation cost (C_{rpc}), is fixed at 0.09(€) [171] and power factor of the DGs are set to 0.8 p.f.

For individual single phase charger at EVCS known quantities are: SAEJ1772-2009 & NEMA 5-20 standards $240V, 16/20A$ single-phase charger, discharging rate = $2.8kW/hr$, charging efficiency (η) = 95% and power factor is ($\cos\phi_{CH}$) = 0.95 [172].

6.5 Results and Discussions

In this section, optimal active and reactive power scheduling of VPPs are carried out on IEEE-25 bus unbalanced system. The segregated effects of with and without the inclusion of unbalanced factor and PAR constraint on optimal active and reactive power scheduling of VPPs is also investigated, so that one may be able to quantify their effects. The candidate site for installation of EVCS and DGs are listed in Table. 6.1.

Table 6.1: Candidate site for EVCS & DGs installation

<table>
<tr><td>DG index</td><td colspan="2">1</td><td colspan="2">2</td><td colspan="2">3</td><td colspan="2">4</td><td colspan="2">5</td></tr>
<tr><td>Bus No.</td><td colspan="2">5</td><td colspan="2">9</td><td colspan="2">13</td><td colspan="2">14</td><td colspan="2">19</td></tr>
<tr><td>Phase</td><td colspan="2">a</td><td colspan="2">a</td><td colspan="2">c</td><td colspan="2">b</td><td colspan="2">b</td></tr>
<tr><td>EVCS index</td><td>1</td><td>2</td><td>3</td><td>4</td><td>5</td><td>6</td><td>7</td><td>8</td><td>9</td><td>10</td></tr>
<tr><td>Bus No.</td><td>4</td><td>8</td><td>14</td><td>23</td><td>24</td><td>3</td><td>18</td><td>12</td><td>19</td><td>6</td></tr>
<tr><td>Phase</td><td>c</td><td>c</td><td>c</td><td>a</td><td>c</td><td>a</td><td>a</td><td>b</td><td>c</td><td>a</td></tr>
</table>

Fig. 6.2 shows the hourly phase, zero sequence component and negative sequence component current at root node with and without the inclusion of unbalanced and PAR constraints. It is observed that from Fig. 6.2, the magnitude of zero and negative sequence current without unbalanced and PAR constraint are in the range of 0.71 p.u to 1.2 p. u whereas, with unbalanced and PAR constraint, zero and negative sequence component currents are restricted to 0.02 p.u, which is almost negligible. Imposing the unbalance and PAR constraint in active and reactive power scheduling of PHEVS and DGs results reduce zero and negative sequence currents at root node. It is also observed that from Fig. 6.2, after imposing unbalance and PAR constraints, the proposed approach can greatly mitigate the current balance at the root node and flatten the 24-hour phase current profile.

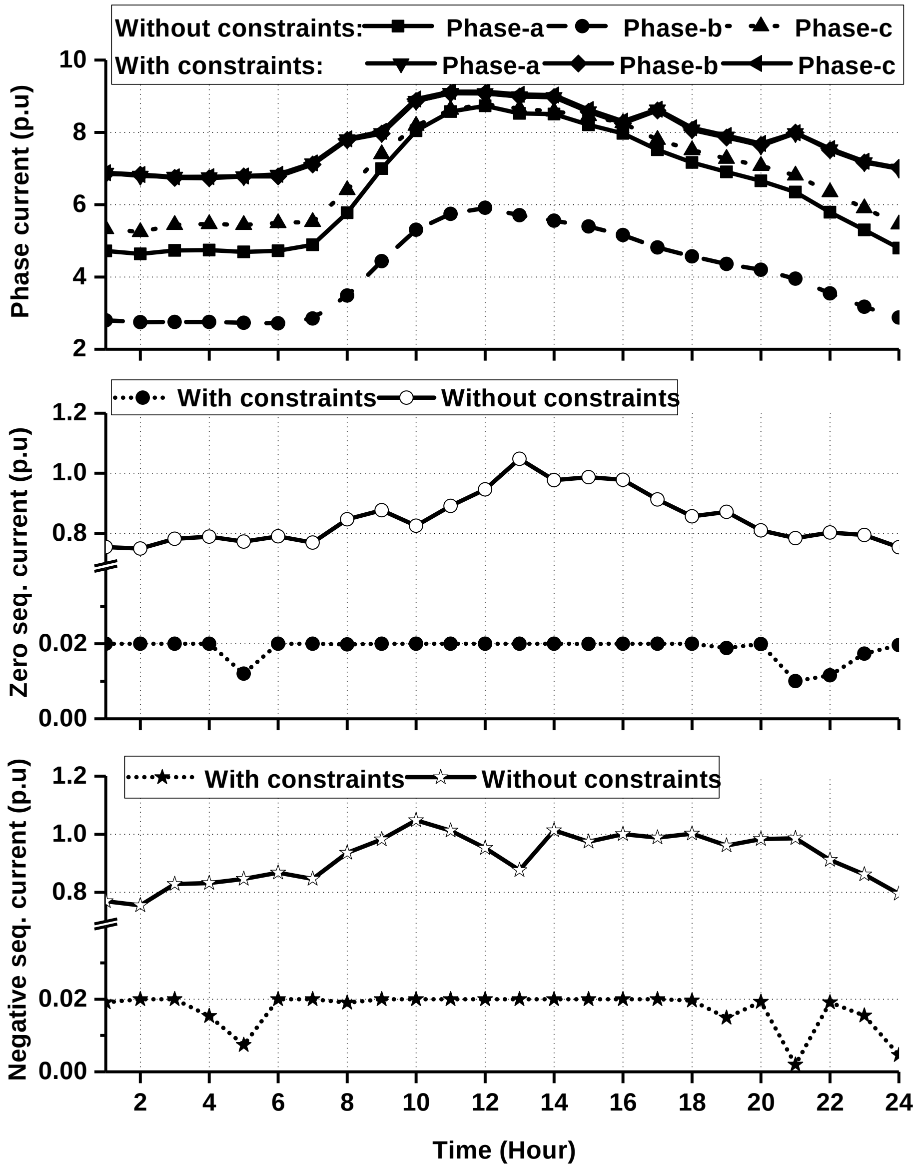

Figure 6.2: Hourly current at root node

Fig. 6.3 & 6.4 shows hourly maximum and minimum PVUI with and without imposing unbalance and PAR constraint in optimal active/reactive power scheduling problem in the distribution system. It is observed that PUVI without employing the voltage phase-balancing constraint results in PVUI already in the acceptable range due to optimal active and reactive power scheduling of PHEVs and DGs. Whereas, after employing the voltage phase-balancing constraint results, the more tighten voltage unbalance range, i.e. ±1.68%. This study reflects the even after optimal scheduling of PHEV and DGs in the unbalanced distribution system; there is still a possibility to tighten more voltage unbalance range after considering additional voltage phase-balancing constraint in the problem formulation.

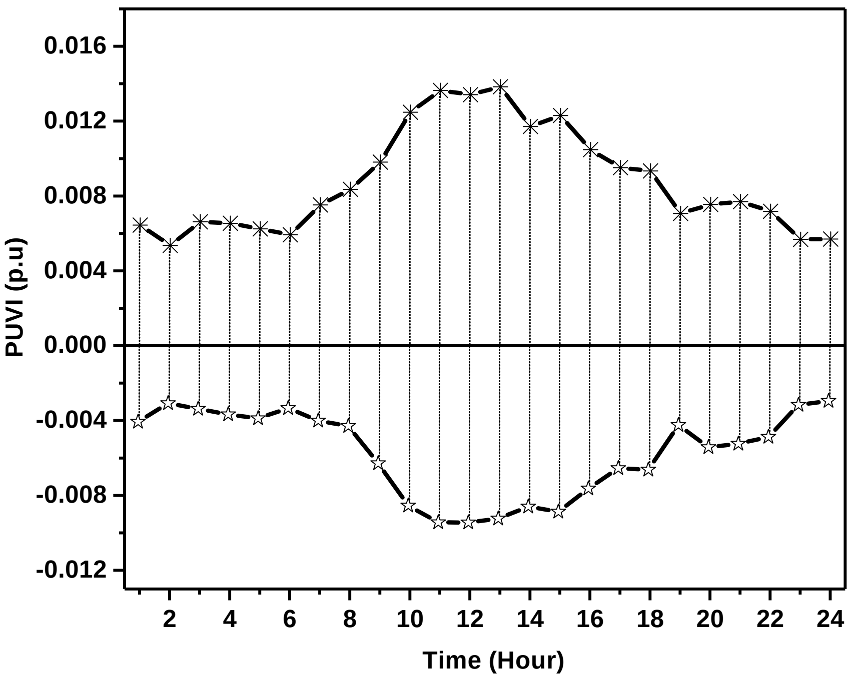

Figure 6.3: Hourly maximum and minimum PVUI with unbalance and PAR constraint

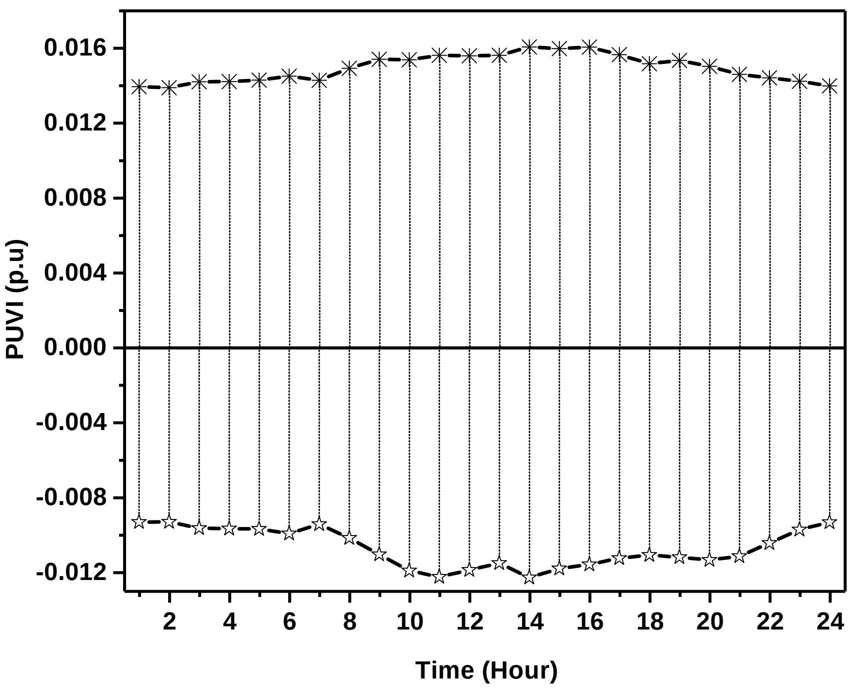

Figure 6.4: Hourly maximum and minimum PVUI without unbalance and PAR constraint

Fig. 6.5 shows a comparison of hourly total active power losses of the system with and without considering the line unbalance and PAR constraints. It is observed from the Fig. 6.5, the active power losses are remarkably higher with unbalance constraint. At this point, it is important to note from the results obtained imposing the unbalance constraint into problem formulation, active power losses increase on the distribution network.

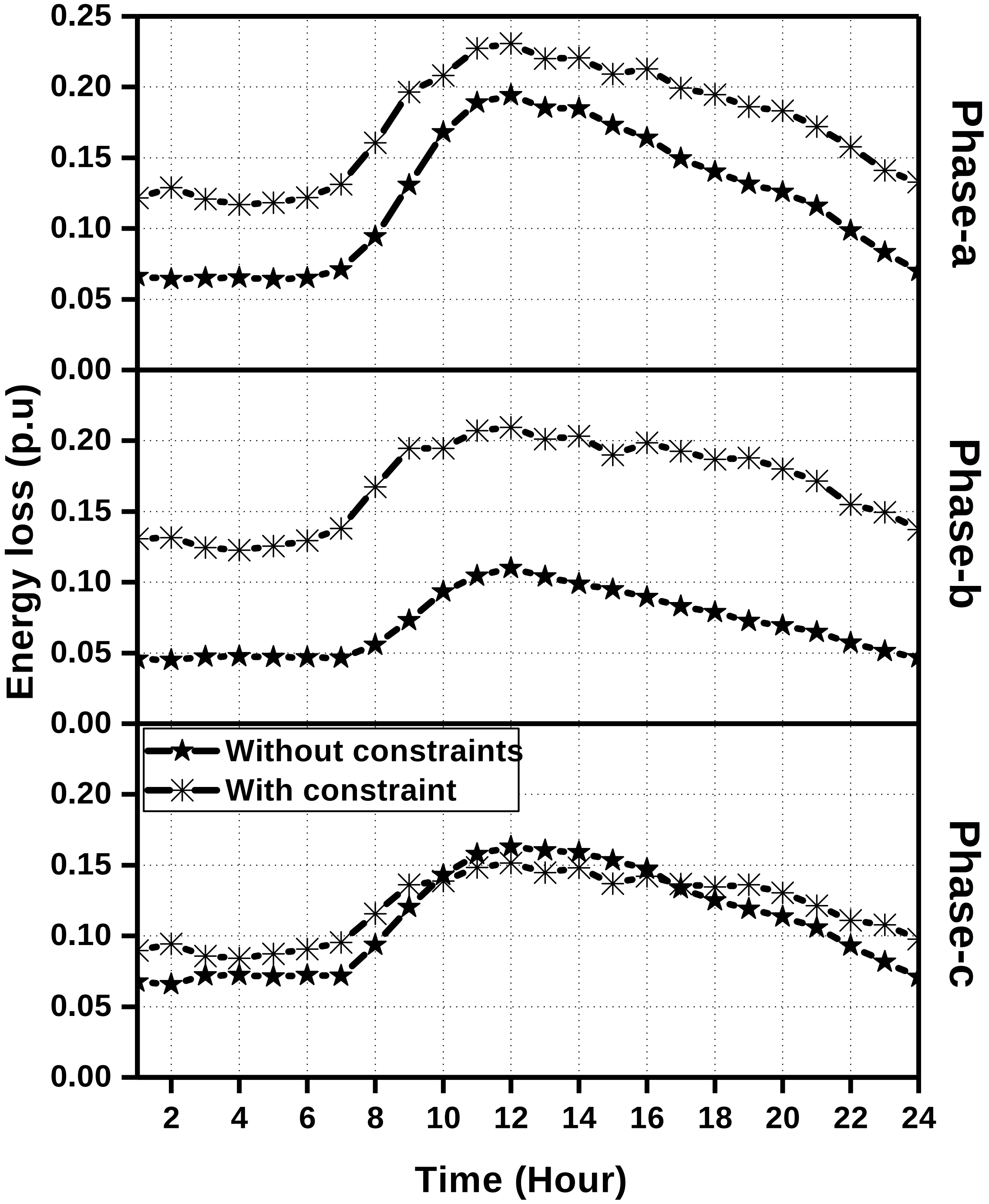

Figure 6.5: Hourly total energy losses

Fig. 6.6 shows the active power scheduling obtained in G2V (shown as positive values) and V2G (shown as negative values) modes. From Fig. 6.6, it can be observed that the without inclusion of line unbalance and PAR constraint, G2V/V2G power pattern responds to reduction in utility cost, i.e. during low tariff period (01:00- 5:00 hours) most of PHEVs are scheduled for charging whereas during high tariff period most of the vehicles are scheduled to discharge into the grid. After imposing the unbalance and PAR constraint on optimal scheduling problem quite different. It can be said that, optimal G2V/V2G scheduling offers the management of PHEVs as storage support to the distribution system to meet techno-economic constraints of unbalance distribution system.

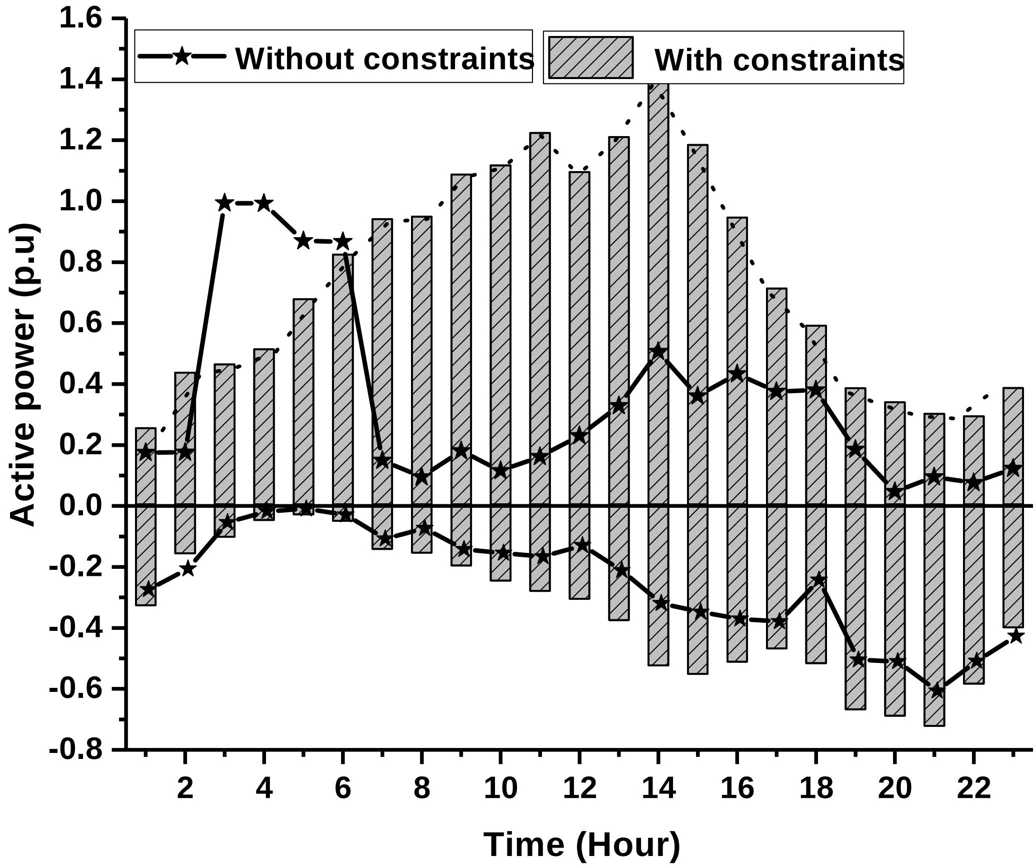

Figure 6.6: Optimal G2V and V2G active power scheduling of PHEVs

Fig. 6.7 shows the reactive power scheduling obtained in G2V (shown as positive values) and V2G (shown as negative values) modes. From Fig. 6.7, it can be observed that the without inclusion of the unbalance and PAR constraints, PHEVs do not absorb reactive power whereas, after considering the unbalance constraint, PHEVs absorb as well as inject reactive power to grid. Moreover, it is also observed that with consideration of unbalance constraint, PHEVs are scheduled to inject reactive power into the grid to miti-

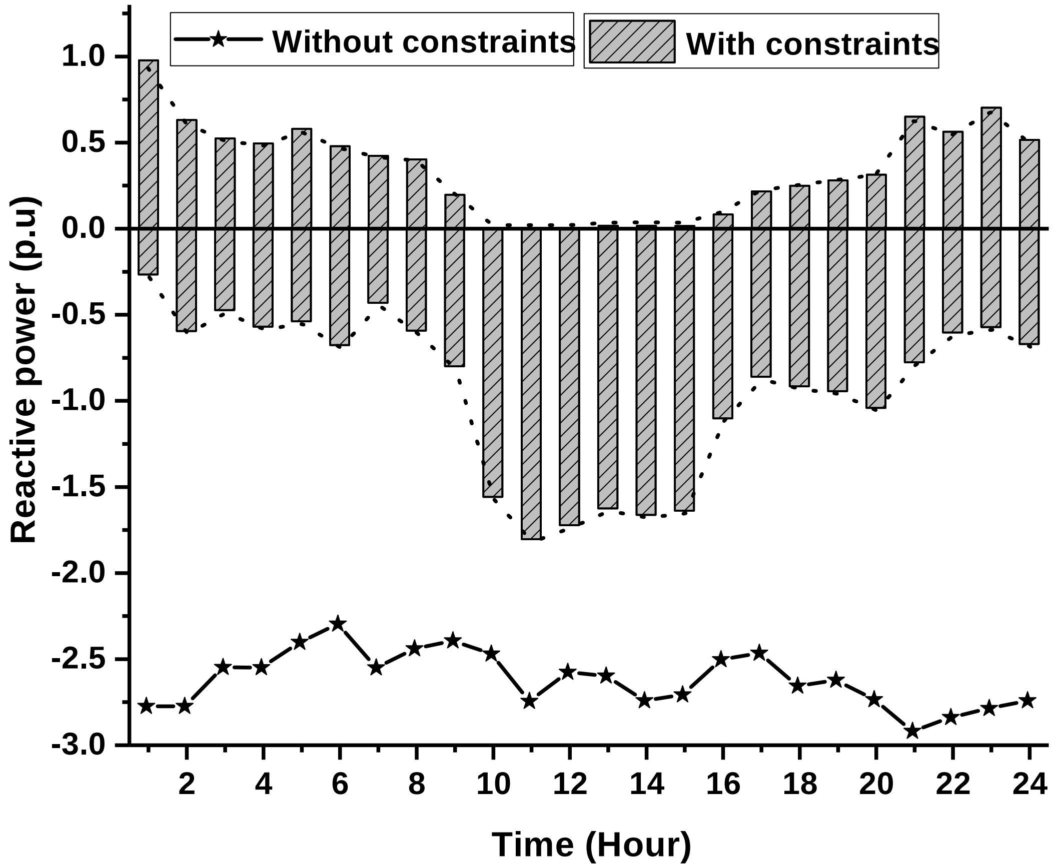

Figure 6.7: Optimal G2V and V2G reactive power scheduling of PHEVs

gate voltage unbalance during peak hours. As a summary, the ability to regulate reactive power by PHEVs, optimal G2V/V2G reactive power scheduling of PHEVs support the unbalance distribution system to achieve voltage balance in the distribution system.

Fig. 6.8 depicts the optimal total active power scheduling of DGs with and without consideration of unbalance and PAR constraints. After examining the scheduling pattern of DGs active power, it is observed that without considering the unbalance constraints all DGs are set to inject maximum power due to the low pricing of DGs unit. while after taking considerations of the unbalance constraints, DGs scheduling significantly change to supports the phase balancing in unbalanced distribution system.

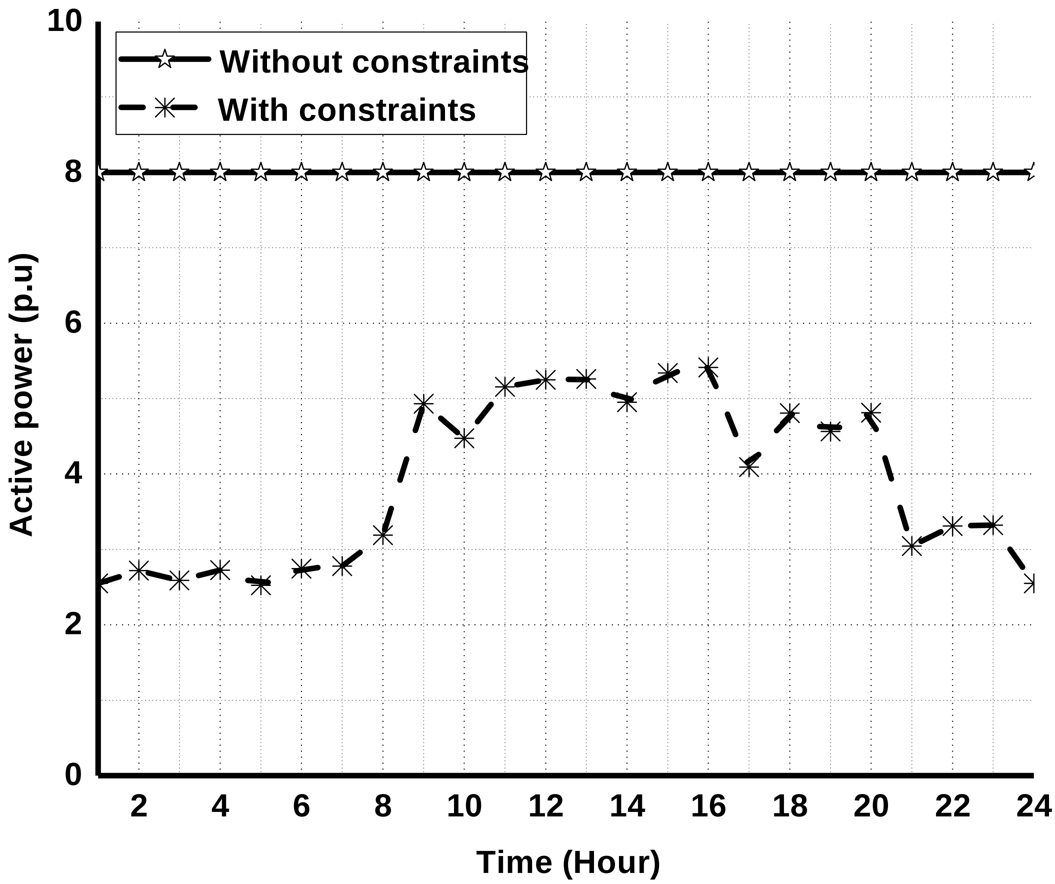

Figure 6.8: Hourly total active power scheduling of DGs

Fig. 6.9 depicts the optimal total reactive power scheduling of DGs with and without consideration of unbalance and PAR. After examining the scheduling pattern of DGs active power, it is observed that without considering the constraints all DGs are set to inject maximum power due to the low pricing of reactive power compensation cost of DGs unit. After taking considerations of unbalance constraints, DGs scheduling significantly change to supports voltage balancing in distribution system. Thus, the unbalance and PAR constraints are important constraints and may pose technical bottleneck in scheduling of DGs.

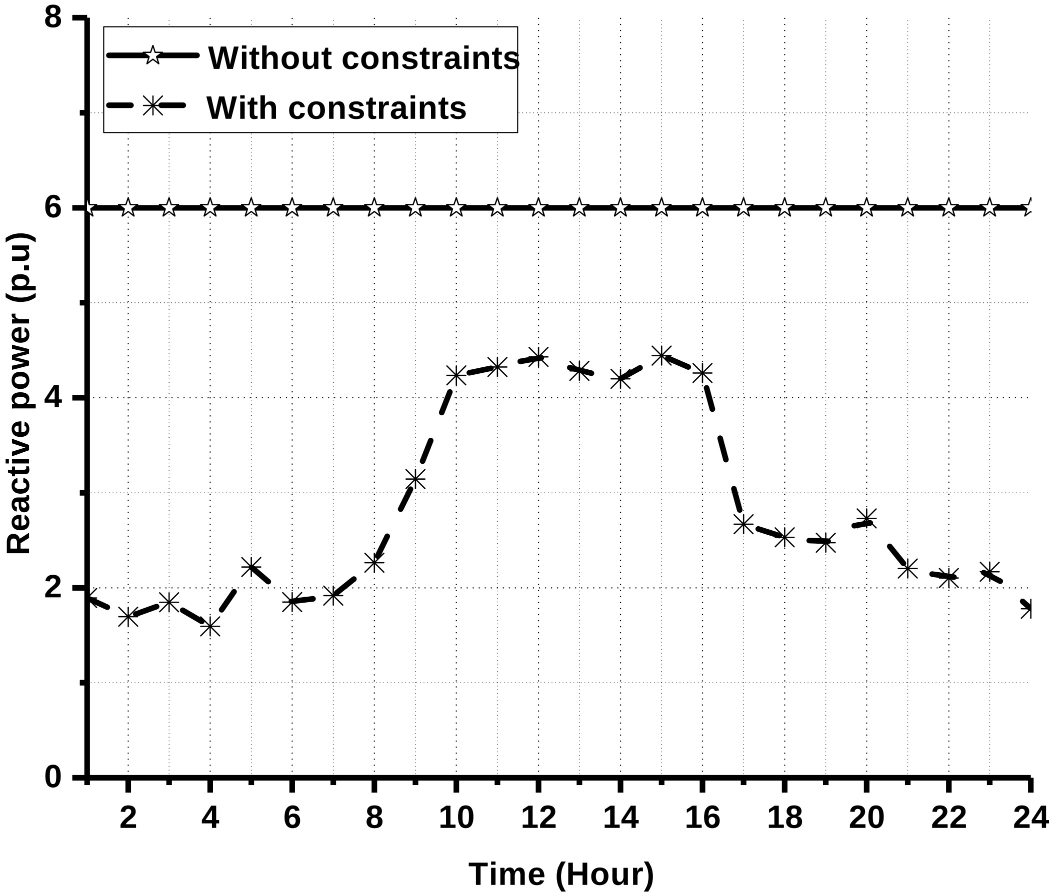

Figure 6.9: Hourly reactive power scheduling of DGs

As a summary, important outcomes with and without consideration of line unbalance, and PAR constraints are compared in Table. 6.2. It is observed that after imposing the unbalance constraints, utility energy cost and energy losses are increased. Improvement in Peak to Average Ratio (PAR) is observed for all the three phases with this approach. Improvement in PAR has been achieved by the scheduling of active power demand among phases by modulating active power of PHEVs and DGs. Whereas, reactive power scheduling of PHEVs and DGs supports distribution system to regulate system voltage. Table. 6.3 shows the pay-off table between unbalance and PAR constraints in terms of cost. Whereas, Table. 6.4 shows the pay-off table between unbalance and PAR constraints in terms of energy losses. It is observed that dependencies between of unbalance factor and PAR is highly non-linear planning problem for VPPs. After investigation, it is also observed that the optimal energy cost and energy losses are 59.202 and 9.031 respectively at 0.025 unbalance factor and at 1.25 PAR.

Table 6.2: Summarized result of important indices

Indices	Without constraint			With constraint		
Cost (€)	49.822			65.479		
I_0^{max} (p.u)	1.05			0.02		
I_2^{max} (p.u)	1.012			0.02		
$PUVI_{min}$ (p.u)	0.016			0.013		
$PUVI_{max}$ (p.u)	0.009			0.002		
	Phase-a	Phase-b	Phase-c	Phase-a	Phase-b	Phase-c
Active power PAR	1.33	1.40	1.24	1.194	1.198	1.2
Active power losses	5.78	3.37	5.36	7.86	7.53	5.54

Table 6.3: Pay-off table for energy cost

PAR	Unbalance Factor					
	0.01	0.015	0.02	0.025	0.03	0.035
1.1	67.334	65.808	65.753	65.447	65.378	65.292
1.15	67.368	65.909	67.284	68.03	67.533	67.14
1.2	67.077	66.351	64.549	63.318	63.234	59.167
1.25	69.09	65.645	64.984	***59.202***	64.15	66.789
1.3	65.832	65.2	65.265	68.695	64.952	62.737
1.35	66.077	66.278	63.023	65.323	62.707	65.084

Table 6.4: Pay-off table for energy losses

PAR	Unbalance Factor					
	0.01	0.015	0.02	0.025	0.03	0.035
1.1	11.460	11.097	11.099	11.081	11.043	11.001
1.15	11.265	10.962	11.386	11.568	11.45	11.465
1.2	11.126	10.961	10.563	10.254	10.139	9.193
1.25	11.806	10.807	10.677	***9.031***	10.356	11.255
1.3	10.789	10.649	10.638	11.721	10.74	9.886
1.35	10.853	10.977	10.046	10.694	9.842	10.693

6.6 Summary

The proposed mathematical framework can be used to obtain the optimal active and reactive power scheduling of PHEVs and DGs in order to achieve current and voltage balance and maintain PAR at desired level in three-phase unbalanced distribution system which aims to minimize operational cost of the VPPs. The scheduling approach is tested on IEEE-25 bus three-phase unbalanced distribution system. The proposed investigation in this chapter also segregated the effects of including and excluding unbalanced factor and PAR constraints on optimal active and reactive power scheduling of VPPs, so that effect of these constraints can be quantified. The analysis of numerical results obtained from proposed investigation are outlined in the following way:

- The magnitude of negative- and zero-sequence currents without unbalance and PAR constraint are in the range of 0.71 p.u to 1.2 p.u. whereas, with unbalance and PAR constraint, negative- and zero-sequence component currents are restricted to 0.02 p.u, from which it is inferred that the phase currents are balanced at root node.
- The proposed investigation ensures that the PVUI is always within the limits ($\pm$ 3%), but there is still a possibility to further tighten PVUI limits (i.e., $\pm$1.68%) after imposing additional voltage unbalance constraints in problem formulation.
- The numerical analysis of results reveals that the maximum PAR reduction is 14.28% at Phase-b after imposing PAR constraints in scheduling problem which will ensure practical availability of peak margins as spinning reserve in distribution system.

The simulation results show that the adopted strategy will force active and reactive power scheduling of PHEVs and DGs to collectively maintain phase balance and PAR at desired level and stick to that scheduling by means of additional operating cost for VPPs.

From the proposed investigation in this chapter, it is also evident that VPPs have an option to tune unbalance factor and PAR to achieve desired techo-economical operation in distribution system. The unbalance factor and PAR are quantified in terms of operational energy cost and energy losses. From results obtained from investigation, it is observed that dependencies of cost and energy losses show that scheduling problem for the VPPs is a highly non-linear problem, which can be inferred by the pay-off table presented between unbalance factor and PAR.